Supercharging with Trivalent Metal Ions in Native Mass Spectrometry

Tawnya G. Flick and **Evan R. Williams**
Department of Chemistry, University of California-Berkeley, Berkeley, CA 94720-1460, USA

Abstract

Addition of 1.0 mM $LaCl_3$ to aqueous ammonium acetate solutions containing proteins in their folded native forms can result in a significant increase in the molecular ion charging obtained with electrospray ionization as a result of cation adduction. In combination with *m*-nitrobenzyl alcohol, molecular ion charge states that are greater than the number of basic sites in the protein can be produced from these native solutions, even for lysozyme, which is conformationally constrained by four intramolecular disulfide bonds. Circular dichroism spectroscopy indicates that the conformation of ubiquitin is not measurably affected with up to 1.0 M $LaCl_3$, but ion mobility data indicate that the high charge states that are formed when 1.0 mM $LaCl_3$ is present are more unfolded than the low charge states formed without this reagent. These and other results indicate that the increased charging is a result of La^{3+} preferentially adducting onto compact or more native-like conformers during ESI and the gas-phase ions subsequently unfolding as a result of increased Coulomb repulsion. Electron capture dissociation of these high charge-state ions formed from these native solutions results in comparable sequence coverage to that obtained for ions formed from denaturing solutions without supercharging reagents, making this method a potentially powerful tool for obtaining structural information in native mass spectrometry.

Keywords

Metalions; Supercharging; Proteins; Native mass spectrometry; Electrospray ionization

Introduction

Electrospray (ESI) ionization is widely used to generate intact multiply charged ions of proteins and protein complexes from aqueous solutions, a technique often referred to as native mass spectrometry (MS) [1–4]. The multiple charging of large molecules that typically occurs with ESI is advantageous for lowering *m/z* values into a range where high performance mass measurements can be made [5, 6]. Increasing analyte charge also increases the sensitivity of mass spectrometers where the signal of an ion is proportional to its charge, such as Orbitrap and Fourier-transform ion cyclotron resonance (FT-ICR) instruments [7, 8].

Several factors affect the extent of analyte charging by ESI, including analyte conformation [9–11], solvent and analyte basicity [12–14], instrumental factors [15, 16], and solvent surface tension [17–19]. Broad charge state distributions of molecular ions centered about

high charge are typically observed from solutions in which proteins are unfolded, whereas narrow distributions at low charge are obtained for proteins and protein complexes formed from solutions in which these molecules have native structures [9–11]. The solution-phase denaturation of proteins as a result of heating or acidifying the bulk ESI solution can be monitored by ESI-MS from shifts in the charge state distribution towards higher charge [10, 11]. Complexation of multivalent metal ions can also increase the charge states of molecular ions formed by ESI [20–23], and has been used effectively to obtain electron capture dissociation (ECD) spectra of small peptides for which multiply protonated ions are not typically formed [21–23].

An effective method to increase the charging observed for many biomolecules is the use of supercharging reagents, such as *m*-nitrobenzyl alcohol (*m*-NBA) [17–19, 24–37]. Originally demonstrated for protein ions formed from denaturing solutions [17–19], this supercharging method is also effective at increasing the charge states of protein and protein complex ions formed from native solutions [24–31]. Supercharging reagents have high boiling points and the concentrations of these reagents increase as ESI droplet evaporation occurs [31, 32]. Enrichment of the supercharging reagent affects many physical properties of the ESI droplet, including the surface tension, temperature, propensities to proton transfer, etc. Results from circular dichroism spectroscopy [29, 31] and hydrogen-deuterium exchange MS [30, 31] indicate the supercharging reagents do not affect protein conformation at the low concentrations typically used in the initial solutions, but can cause chemical and/or thermal denaturation of the protein in the ESI droplet as the concentration of these reagents is increased. Proteins that have lost some or all of their native structures can carry away more charge and the charge enhancement from the denaturing effect is greater than the effect of the lower surface tension [28].

High charge state ions typically dissociate more readily to produce structurally useful information, which can lead to higher sequence coverage in tandem mass spectrometry experiments with peptides and proteins [38, 39]. This is especially the case with electron capture or transfer dissociation where extensive sequence coverage can be obtained from the high charge state molecular ions of proteins that are typically formed from denaturing solutions [40, 41]. However, information about the native conformation, protein–substrate interactions, or stoichiometry of macromolecular assemblies can be lost under denaturing conditions. Supercharging improves the ability to combine "top-down" tandem mass spectrometry with native mass spectrometry, which can be used to read out encoded information about conformations and conformational changes that occur in solution, such as solution-phase H/D exchange rates [30] and other labeling strategies, or identifying protein–ligand binding sites directly from fragmentation of an intact complex [36].

The charge states of proteins generated by ESI from unbuffered aqueous solutions can also be increased by introducing acid vapor into the drying gas of an ESI interface [42]. Addition of HCl acid vapor into the drying gas resulted in an increase in the maximum charge state of cytochrome *c* by 10 and a shift in the average state from 8.9 to 15.4 compared to that obtained when no acid vapor was introduced [42]. The acid vapor lowers the pH of the ESI droplet and acid denaturation of the protein occurs, resulting in higher ion charge states in the mass spectrum [42]. An electrothermal supercharging method to generate high charge state protein ions with ESI from buffered aqueous solutions in which the proteins have native structures was recently introduced [43]. ESI mass spectra resembling those obtained from denaturing solutions, where the maximum extent of charging can exceed the number of basic sites in the molecule, can be obtained with this method [43]. The effectiveness of this method to increase charging depends on a number of different factors, but ESI mass spectra resembling those measured from standard native or denatured solutions can be reversibly obtained simply by toggling the electrospray voltage between low and high values [43]. This

method has the advantage over acidification of the ESI droplets in that it can be used with aqueous solutions that have high buffer capacity [43].

Here, addition of millimolar concentrations of La^{3+} to aqueous protein-containing solutions is shown to increase the extent of protein charging by ESI as a result of La^{3+} adduction onto native protein conformers. The enhanced protein charging via La^{3+} adduction is slightly lower than that obtained from aqueous ammonium acetate solutions that contain the supercharging reagent m-NBA, but both m-NBA and $LaCl_3$ can be used in combination to readily form charge states in excess of the number of basic sites in the protein. ECD of high charge states generated by trivalent metal ion supercharging from aqueous solutions results in improved fragmentation efficiency and sequence coverage compared with that obtained from the highest charge state formed from aqueous solutions without La^{3+}.

Experimental

Mass Spectrometry

Experiments were performed using a 9.4 T FT-ICR mass spectrometer equipped with an external ESI source [44]. Bovine ubiquitin, bovine cytochrome c, chicken egg white lysozyme, $LaCl_3$, m-nitrobenzyl alcohol (m-NBA), methanol, acetic acid, and ammonium acetate were all purchased from Sigma Aldrich (St. Louis, MO, USA). Stock solutions containing 10 μM protein were prepared in either water with 5 mM ammonium acetate or with 48.5/48.5/3.0 methanol/water/acetic acid (vol/vol/vol). A small volume of sample solution (~2–10 μL) is loaded into a borosilicate capillary (1.0 mm o.d./0.78 mm i.d.; Sutter Instruments, Novato, CA, USA) that is pulled to a tip with an inner diameter of ~2 μm (model P-87 capillary puller; Sutter Instruments). A grounded platinum wire is inserted into the solution and the capillary is positioned ~2 mm away from the source inlet capillary to which a potential of −800 to −1200 V is applied. Ions are accumulated in an external hexapole ion trap for 2.0 s and are subsequently injected into the ion cell, and this process is repeated two additional times in order to load the ion cell. For ECD experiments, the precursor ion of interest is isolated using stored waveform inverse Fourier transforms (SWIFTs) [45] with a 2 kHz or wider window around the precursor. Electrons from a heated dispenser cathode (Heatwave Labs, Watsonville, CA, USA) that is mounted axially from the cell center are introduced into the ion cell 100 ms after ion isolation by changing the cathode housing potential from +10 V to either −0.40 or −0.65 V for 100 ms. Ions are detected 1.0 s after electron irradiation. EC efficiency (Eff_{EC}) is calculated using Equation 1

$$Eff_{EC} = \frac{\Sigma I_{fragment} + \Sigma I_{reduced}}{I_{precursor} + \Sigma I_{reduced} + \Sigma I_{fragment}} \quad (1)$$

where $I_{precursor}$, $I_{fragment}$, and $I_{reduced}$ are ion abundances of the precursor remaining after the ECD event, the fragments, and the reduced precursors, respectively. Fragmentation efficiency (Eff_{frag}) is calculated using Equation 2

$$Eff_{frag} = \frac{\Sigma I_{fragment}}{I_{precursor} + \Sigma I_{reduced} + \Sigma I_{fragment}} \quad (2)$$

The measured ion abundances were normalized for charge, but effects of any m/z-dependent detection efficiency or isotopes not included in these calculations were not taken into account. Uncertainties for electron capture and fragmentation efficiencies are reported as ± one standard deviation of three replicate measurements. Each measurement was repeated with a different SWIFT for isolation with a window between two to four kHz around the precursor. Off-resonance excitations can transfer kinetic energy into ions, but this effect

decreases as the frequency of the excitation becomes more off-resonance [46]. Changing the SWIFT window between these values changes the extent of off-resonance excitation that occurs [45], but there was no significant effect on either the electron capture or fragmentation efficiencies. These results indicate that the SWIFT isolations do not measurably affect the overlap of the precursor ions and the electrons. The reported signal-to-noise ratios (S/N) are determined directly from the mass spectral data and are not normalized for ion charge.

Circular Dichroism

Circular dichroism (CD) spectra were acquired on a Jasco model 810 spectropolarimeter (JASCO, Inc., Easton, MD, USA) from solutions containing 20 μM ubiquitin in denaturing solution conditions (48.5/48.5/3 methanol/water/acetic acid) or water with 5.0 mM ammonium acetate either with no additional additive or 1.0 mM to 5.0 M $LaCl_3$. Samples were transferred to a 1.0 cm quartz cuvette with constant mixing using a Teflon stir bar while performing a wavelength scan analysis from 210 to 250 nm.

Ion Mobility

Ion mobility experiments were performed using a Synapt G2 High Definition mass spectrometer (Waters, Milford, MA, USA) equipped with a Z-spray ion source. Ions are formed by ESI as described above using a platinum wire potential of 1.0 to 1.5 kV. The sample and extraction cone potentials were 40 and 3 V, respectively. The traveling wave ion mobility cell was operated with a constant wave velocity of 700 m/s, wave height of 40 V, helium flow rate of 180 mL/min, and IMS (N_2) flow rate of 90 mL/min. The time of flight mass analyzer was operated in sensitivity mode ("V"). Drift times were converted to a collision cross section (ccs) scale using the procedure outlined by Robinson and coworkers [47, 48] with ubiquitin (9+ through 13+), cytochrome *c* (13+ through 18+), and myoglobin (16+ through 22+) formed from denaturing solutions as calibrant ions. An average ccs was obtained for a given charge state of ubiquitin by weighting the ccs for each conformation by peak area.

Results and Discussion

Trivalent Metal Ion Supercharging in Aqueous Solutions

The 5+ charge state of ubiquitin is the most abundant ion produced by ESI (aqueous 5.0 mM ammonium acetate), and the average and maximum charge states are 5.2 and 7, respectively (Figure 1a). With 1.0 mM $LaCl_3$ added to this solution, the average (7.6) and maximum (11) charge states are significantly higher (Figure 1b). More La^{3+} ions adduct to the higher charge state ions. The average number of La^{3+} adducts increases from 1.7 to 3 for the 6+ and 11+ charge states, respectively. About 12 % of the 6+ molecular ions are fully protonated whereas all ions of the 11+ charge state have La^{3+} bound. Similar results were also obtained from ESI of an aqueous solution containing 1.0 mM $EuCl_3$ (data not shown), suggesting that the binding of these metal ions to the protein is not specific. In contrast, ESI of an aqueous solution of ubiquitin containing 1.0 mM NaCl results in no significant change to the average charge state (5.0), and Na^+ adduction occurs more substantially to the lower charge state ions (data not shown), a result consistent with previous reports [49, 50]. The greater adduction of La^{3+} to higher charge states of ubiquitin suggests that the higher charge states that are formed with $LaCl_3$ are due to the added charge of these trivalent metal ions when they adduct to ubiquitin which is folded in solution.

To compare the extent of charge enhancement obtained from native solutions with $LaCl_3$ to conventional supercharging reagents [24–31], an ESI mass spectrum of an aqueous solution of ubiquitin with 1.0 % *m*-NBA was obtained under identical conditions (Figure 1c). The

charge state distribution is slightly broader than that obtained with LaCl$_3$ and it is centered about 9+ with an average charge state of 8.5. The maximum charge state (11) that is formed is the same for both m-NBA or LaCl$_3$, but with m-NBA, the average charge state is one higher and the abundance of the maximum charge state is greater.

To determine whether the combination of trivalent metal ion adduction and m-NBA results in more charging than either reagent individually, an ESI mass spectrum of ubiquitin from an aqueous solution containing both 1.0 % m-NBA and 1.0 mM LaCl$_3$ was obtained (Figure 1d). The average (9.8) and maximum (14) charge states are greater than those obtained with either LaCl$_3$ or m-NBA alone. Higher charge states have more La^{3+} adduction, as occurred without m-NBA. The 12+ to 14+ charge states all have La^{3+} bound, whereas La^{3+} is adducted to only 9.5 % of the 7+ charge state ions. Ubiquitin has 13 basic sites consisting of 12 basic amino acids (H, R, and K) and the N-terminus. Thus, formation of the 14+ charge state corresponds to charging greater than the number of basic sites in the protein despite formation of these ions from an aqueous solution in which ubiquitin has a folded structure.

Similar results were obtained for bovine cytochrome c, a larger protein with a higher isoelectric point than ubiquitin. The average and maximum charge states of cytochrome c in an ESI mass spectrum from an aqueous solution with 5.0 mM ammonium acetate are 6.9 and 8, respectively (Figure 1e). With 1.0 mM LaCl$_3$, the average and maximum charge states in the ESI mass spectrum increase to 8.9 and 13, respectively (Figure 1f). The average (10.3) and maximum (14) charge states with 1.0 % m-NBA are slightly higher than those obtained with 1.0 mM LaCl$_3$ (Figure 1g). With both m-NBA and LaCl$_3$, the average (12.5) and maximum (17) charge states are 5.6 and 9 more charges, respectively, than those formed from ammonium acetate alone (Figure 1h).

To determine the extent to which intramolecular disulfide bridges, which reduce the conformational flexibility of a protein, can affect the charge enhancement by LaCl$_3$, an ESI mass spectrum of an aqueous solution (5.0 mM ammonium acetate) containing 10 μM lysozyme and 1.0 mM LaCl$_3$ was obtained (Figure S1). With 1.0 mM LaCl$_3$, the average and maximum charge states increase from 8.0 to 9.7 and 10 to 12, respectively, compared with those obtained from the solution containing ammonium acetate alone. An aqueous solution containing both 1.0 mM LaCl$_3$ and 1.0 % m-NBA results in average and maximum charge states of 11.8 and 20, respectively. Lysozyme has 19 basic sites, and the formation of the 20+ charge state indicates that charge states greater than the number of basic sites can be generated from a native solution even for a protein that is conformationally constrained by disulfide bonds.

Effect of Supercharging Additives on S/N

The effects of LaCl$_3$ and m-NBA, individually and combined, on the signal-to-noise ratios (S/N) of the most abundant ion and total ion abundance for ubiquitin, cytochrome c, and lysozyme are shown in Table 1. There is little to no adverse affect on ESI signal for any of these proteins with 1.0 % m-NBA, consistent with previous results [18]. Similarly, 1.0 mM LaCl$_3$ has little effect on the total ion abundance, but does lower the S/N for the most abundant ion. The S/N of the most abundant ion is 39 %, 13 %, and 37 % lower for ubiquitin, cytochrome c, and lysozyme, respectively, with 1.0 mM LaCl$_3$ compared with ammonium acetate alone, as a result of ion abundance being distributed into multiple peaks with varying numbers of La^{3+} adducts. With both m-NBA and LaCl$_3$, the total ion abundance for all three proteins is reduced compared with ammonium acetate alone. Similar to results with just LaCl$_3$, the S/N of the most abundant ion is significantly reduced (~2–9×) because ion abundance is distributed over varying numbers of La^{3+} adducts.

Effect of La^{3+} on Protein Conformation

High charge state protein ions can be formed by ESI from solutions in which the protein is unfolded, or when protein unfolding occurs in the ESI droplet [26–31, 42]. The effect of LaCl$_3$ on protein conformation in solution was investigated using circular dichroism (CD). Far-UV CD spectra (210–250 nm), which probes the α-helical and β-sheet content of a protein, were acquired for ubiquitin in a denaturing solution, 5.0 mM ammonium acetate solution, and 5.0 mM ammonium acetate solution containing between 1.0 mM to 5.0 M LaCl$_3$ (Figure 2a). The CD signal in this spectral region is the same with and without LaCl$_3$ for concentrations up to 1.0 M, indicating that there is no measurable change in the secondary structure of ubiquitin. With 5.0 M LaCl$_3$, the CD spectrum is distinctly different, indicating that the secondary structure changes at this high salt concentration. The CD spectrum of denatured ubiquitin has a notable decrease in ellipticity at 220 nm compared with that obtained for the folded form from native solutions, which is consistent with an increase in α-helical content characteristic of the denatured A-state form of ubiquitin [51].

Ion mobility experiments were performed to investigate how La^{3+} adduction affects the conformations of the resulting gaseous ubiquitin ions. There are multiple conformers for many charge states of ubiquitin (Figure S2), consistent with previous studies [52, 53]. To simplify comparisons, the average ccs for each charge state was determined by weighting each feature in the drift profile by peak area. The average ccs as a function of the charge state of ubiquitin for fully protonated ions generated from native and denaturing solutions, and for ions with two or three La^{3+} adducts formed from aqueous solutions containing LaCl$_3$ is shown in Figure 2b. For the fully protonated ions generated from a denaturing solution, the average ccs increases with increasing charge, as previously reported [52, 53]. For aqueous solutions containing 1.0 mM LaCl$_3$, the average ccs of ubiquitin ions with two or three La^{3+} adducts also increases with increasing charge state, and the 8+ to 14+ La^{3+} adducted ubiquitin ions have more elongated conformations compared with the fully protonated 5+ and 6+ charge states formed from ammonium acetate alone. However, the average ccs values of the La^{3+} adducted ions are consistently smaller than the corresponding protonated form with the same charge state generated from either a native or denaturing solution. The more compact structures may be a result of strong salt-bridge or charge-solvation interactions between the metal ion and deprotonated residues or polarizable atoms in the protein [54] or it may be due to lower charge–charge repulsion as a result of fewer charge carriers that are more highly charged but are spaced further apart compared with the fully protonated ion. The CD data indicate that 1.0 mM LaCl$_3$ does not denature ubiquitin in the initial solution, but the ion mobility experiments show that La^{3+}-bound high charge state ions (8+ to 14+) formed from this solution have more elongated conformations than the 5+ and 6+ charge states formed without LaCl$_3$. This indicates that the presence of La^{3+} causes ubiquitin to unfold during the late stages of the electrospray process or in the gas phase.

Effects of Trivalent Metal Ion Supercharging on ECD

High charge state ions typically dissociate more readily, which can increase the structural information obtained in tandem MS experiments [30, 38–41]. To determine how ECD sequence coverage is affected by supercharging with either La^{3+} adduction, *m*-NBA, or a combination of both, ECD spectra of the highest charge state of ubiquitin that could be isolated with sufficient S/N (> ~1000) to observe most fragments were obtained from an ammonium acetate solution (6+) and ammonium acetate solutions containing LaCl$_3$ (9+), *m*-NBA (10+), or both supercharging additives (12+). ECD sequence coverage depends on a number of different factors, including the ion–electron interaction time, electron current, and the number of scan averages. Here, ECD conditions were optimized for (ubiquitin+6H)$^{6+}$, and these same conditions were used for all other ions to directly compare the Eff$_{EC}$, Eff$_{frag}$, and sequence coverage between different ion charge states. ECD of (ubiquitin+6H)$^{6+}$

formed from a 5 mM ammonium acetate aqueous solution results primarily in the formation of the 5+ and 4+ reduced precursors. Fragmentation occurs close to the N- and C-termini (Figure 3a) with no fragmentation between residues 23 and 59, suggesting that residues within this region are involved in extensive noncovalent interactions [40, 41]. ECD of (ubiquitin+3La)$^{9+}$ results in additional fragmentation in the middle of the protein (Figure 3b). The electron capture and fragmentation efficiencies for (ubiquitin+3La)$^{9+}$ are 9 % and 21 %, respectively, higher than the values obtained for the fully protonated 6+ ion (Table 2). The sequence coverage obtained from the ECD spectrum of (ubiquitin+6H)$^{6+}$ is 33 %, whereas that for (ubiquitin+3La)$^{9+}$ is 63 %. These results indicate the significant advantage in using LaCl$_3$ to increase the charge state of protein ions to obtain enhanced sequence coverage and electron capture efficiency for ECD of protein ions formed from native solutions.

Extensive fragmentation occurs throughout the protein from ECD of (ubiquitin+10H)$^{10+}$ formed from an aqueous solution containing 1.0 % m-NBA (Figure 3c), and 55 % sequence coverage is obtained. (ubiquitin+3La)$^{9+}$ has both an ~11 % smaller average ccs and a lower charge state than (ubiquitin+10H)$^{10+}$, yet greater sequence coverage is obtained for the La^{3+} adducted ion. ECD of (ubiquitin+9 H+La)$^{12+}$ formed from a solution with both 1.0 % m-NBA and 1.0 mM LaCl$_3$ results in even more extensive fragmentation along the backbone of the protein (Figure 3d), from which 76 % sequence coverage is obtained. Thus, a 2.3-fold increase in sequence coverage is obtained from the high charge state ion that is formed with both supercharging reagents compared with the ion formed from native solutions that do not contain these reagents. ECD data of (ubiquitin+6H)$^{6+}$, (ubiquitin+3La)$^{9+}$, (ubiquitin +10H)$^{10+}$, and (ubiquitin+9H+La)$^{12+}$ combined results in 89 % sequence coverage for these ions that are formed from native solutions.

Similar improvements in sequence coverage occurred from ECD of high charge state ions of cytochrome c formed from ammonium acetate solutions containing either m-NBA, LaCl$_3$ or both compared with data obtained without supercharging additives. The 7+ and 6+ reduced precursors are predominantly produced by ECD of (cytochrome c+8H)$^{8+}$ formed from an ammonium acetate solution, and 30 % sequence coverage is obtained (Figure 4a). ECD of (cytochrome c+7H+La)$^{10+}$ formed from an aqueous solution containing 1.0 mM LaCl$_3$ results in more extensive fragmentation throughout the protein (Figure 4b); 53 % sequence coverage is obtained, whereas only 43 % sequence coverage is obtained from ECD of (cytochrome c+12H)$^{12+}$ generated from an aqueous solution containing 1.0 % m-NBA (Figure 4c). Using both m-NBA and LaCl$_3$, ECD of (cytochrome c+11H+La)$^{14+}$ results in 56 % sequence coverage (Figure 4d). The sequence coverage from the combined ECD data for all four of these protein ions formed from native solutions is 76 %, more than double the sequence coverage obtained without these reagents.

Effect of Cross Section and Trivalent Metal Ion on ECD

Results presented here and from earlier studies [30, 38–41] show that greater sequence coverage is often obtained from dissociation of high charge state protein ions, which tend to have elongated conformations compared to low charge state protein ions with compact structures; (ubiquitin+2La)$^{6+}$ has an ~14 % smaller average ccs than that of (ubiquitin +6H)$^{6+}$, and the EC efficiency, fragmentation efficiency, and sequence coverage are 7 %, 19 %, and 8 % lower, respectively, for (ubiquitin+2La)$^{6+}$ compared with (ubiquitin+6H)$^{6+}$ (Table 2). However, greater sequence coverage was not always obtained from ECD of a protein ion with a higher charge state and larger ccs. For example, ECD of (ubiquitin +3La)$^{9+}$ results in 8 % higher sequence coverage than (ubiquitin+10H)$^{10+}$, even though the 9+ ion has one less charge and ~11 % smaller average ccs. Similarly, (cytochrome c+La +3H)$^{10+}$ has a ~9 % smaller average ccs than (cytochrome c+12H)$^{12+}$, yet ECD of the smaller, less highly charged La^{3+} bound ion results in 10 % higher sequence coverage.

These results indicate that the ccs and charge state of an ion are not the only factors in determining the extent of sequence coverage, and other characteristics such as ion shape [55] must play a significant role.

Trivalent Metal Ion Supercharging with Denaturing Solution

To determine the extent to which La^{3+} adducts to denatured proteins in solution, an ESI mass spectrum of ubiquitin from a denaturing solution (48.5/48.5/3 methanol/water/acetic acid) containing 1.0 mM $LaCl_3$ was obtained (Figure 5b). Both the average (10.3) and maximum (13) charge states are essentially the same for the solutions with and without $LaCl_3$ (Figure 5a). More La^{3+} adduction to lower charge state ions occurs, which is in striking contrast to results for aqueous solutions where La^{3+} adduction increases with increasing charge state. The percentage of the 7+ and 12+ charge states that have La^{3+} adducted are 79 % and 32 %, respectively. Similar results were obtained from the denaturing solution containing $LaCl_3$ when the metal salt was added to the protein-containing solution either before or after the denaturing reagents (methanol and acetic acid), indicating that the metal ions do not kinetically trap the protein into less stable structures in these experiments. With 1.0 % m-NBA, the average charge state increases from 10.1 to 11.8 (Figure 5c) and the maximum charge state formed is 14+. With both 1.0 % m-NBA and 1.0 mM $LaCl_3$, the 16+ charge state is formed, which is three more charges than the total number of basic sites in this protein. The charge state distribution is centered about the 13+ and the average charge state is 13.4. These results demonstrate that trivalent metal ion supercharging in denaturing solutions using ESI can be used to produce higher charge states of proteins than have previously been observed.

An ECD mass spectrum of (ubiquitin+11H+La)$^{14+}$ formed from a denaturing solution containing 1.0 % m-NBA and 1.0 mM $LaCl_3$ was acquired and the resulting fragments are shown in Figure 6b. The low S/N of (ubiquitin+14H)$^{14+}$ (~20) formed from the denaturing solution with 1.0 % m-NBA precludes a direct comparison to ECD of the fully protonated 14+ charge state, but fragments formed by ECD of (ubiquitin+13H)$^{13+}$ are shown in Figure 6a. The electron capture and fragmentation efficiencies of (ubiquitin+11H+La)$^{14+}$ are only slightly greater, 5% and 4 %, respectively, than for (ubiquitin+13H)$^{13+}$. The sequence coverage obtained under these conditions for both ions was 68 %. However, many of the ECD fragments formed from both ions are unique, resulting in 85 % sequence coverage when the data from both ions are combined. These data indicate that ECD of high charge states formed from denaturing solutions containing both m-NBA and $LaCl_3$ can significantly improve the sequence coverage.

Mechanism of Charging via La^{3+} Adduction

The CD results show that the secondary structure content of ubiquitin is not affected in solutions with up to 1.0 M $LaCl_3$, but denaturation occurs with 5.0 M $LaCl_3$. For denaturation to occur in the ESI droplet, the $LaCl_3$ concentration must increase by more than a 1000-fold from the initial 1.0 mM concentration. By comparison, a ~×5 enrichment of the supercharging reagent dimethyl sulfoxide occurs in the ESI droplet to produce supercharging [31]. Minimal La^{3+} adduction occurs for protein ions formed from denaturing solutions, and more La^{3+} adducts to lower charge state ions. In striking contrast, significant La^{3+} adduction to protein ions generated from native solutions occurs, and more La^{3+} adducts to higher charge state ions. These results suggest that La^{3+} preferentially adducts to native or native-like protein conformers during ESI. The higher charge state La^{3+} bound ubiquitin ions (8+ to 14+) have more elongated conformations than low charge state ions (5+ and 6+) formed from native solutions without $LaCl_3$. These results suggest that substantial adduction of La^{3+} onto compact conformers of ubiquitin during ESI results in

protein ions with higher charge, which subsequently adopt more unfolded gas-phase conformations, presumably due to higher Coulombic repulsion.

Conclusions

LaCl$_3$ can significantly increase the average and maximum charge states of protein ions formed by ESI from native solutions. Charge states greater than the number of basic sites in the protein can be produced from either aqueous solutions in which the protein has a native folded structure, or denaturing solutions that contain both La^{3+} and *m*-NBA, even for a protein that is conformationally constrained due to native disulfide bonds. This method may be useful for increasing charging in LC/MS experiments where LaCl$_3$ could either be added to the mobile phase or it could be added post-column as has been reported for other supercharging reagents [56].

Better ECD sequence coverage can be obtained from the high charge state protein ions formed as a result of La^{3+} adduction, making the information content of ECD of protein ions formed from native solutions comparable to that obtained from denaturing solutions. Addition of 1.0 mM LaCl$_3$ to aqueous solutions does not adversely affect the total protein ion abundance generated by ESI, but can lower the S/N of the most abundant ion owing to the distribution of signal into ions with various numbers of La^{3+} adducts. However, the improved fragmentation efficiency and sequence coverage obtained for the high charge state La^{3+} adducted ions more than compensates for the reduced precursor abundance. These results indicate that trivalent metal ion supercharging can substantially increase the fragmentation of protein ions formed from native solutions, and should reduce the need to denature proteins prior to tandem MS analysis.

Supplementary Material

Refer to Web version on PubMed Central for supplementary material.

Acknowledgments

References

1. van den Heuvel RH, Heck AJR. Native protein mass spectrometry: From intact oligomers to functional machineries. Curr. Opin. Chem. Biol. 2004; 8:519–526. [PubMed: 15450495]

2. Heck AJR. Native mass spectrometry: A bridge between interactomics and structural biology. Nat. Methods. 2008; 5:927–933. [PubMed: 18974734]

3. Kaddis CS, Loo JA. Native protein MS and ion mobility: Large flying proteins with MS. Anal. Chem. 2007; 79:1778–1784. [PubMed: 17375392]

4. Barrera NP, Robinson CV. Advances in the mass spectrometry of membrane proteins: From individual proteins to intact complexes. Annu. Rev. Biochem. 2011; 80:247–271. [PubMed: 21548785]

5. Loo JA, Quinn JP, Ryu SI, Henry KD, Senko MW, McLafferty FW. High-resolution tandem mass-spectrometry of large biomolecules. Proc. Natl. Acad. Sci. U. S. A. 1992; 89:286–289. [PubMed: 1309610]

6. Marshall AG, Hendrickson CL. Charge reduction lowers mass resolving power for isotopically resolved electrospray ionization fourier transform ion cyclotron resonance mass spectra. Rapid Commun. Mass Spectrom. 2001; 15:232–235.

7. Marshall AG, Hendrickson CL. High-resolution mass spectrometers. Annu. Rev. Anal. Chem. 2008; 1:579–599.

8. Perry RH, Cooks RG, Noll RJ. Orbitrap mass spectrometry: Instrumentation, ion motion and applications. Mass Spectrom. Rev. 2008; 27:661–699. [PubMed: 18683895]

9. Testa L, Brocca S, Grandori R. Charge-surface correlation in electrospray ionization of folded and unfolded proteins. Anal. Chem. 2011; 83:6459–6463. [PubMed: 21800882]

10. Chowdhury SK, Katta V, Chait BT. Probing conformational-changes in proteins by mass-spectrometry. J. Am. Chem. Soc. 1990; 112:9012–9013.

11. Wang GB, Abzalimov RR, Kaltashov IA. Direct monitoring of heat-stressed biopolymers with temperature-controlled electrospray ionization mass spectrometry. Anal. Chem. 2011; 83:2870–2876. [PubMed: 21417416]

12. Williams ER. Proton transfer reactivity of large multiply charged ions. J. Mass Spectrom. 1996; 31:831–842. [PubMed: 8799309]

13. Loo RRO, Smith RD. Proton-transfer reactions of multiply-charged peptide and protein cations and anions. J. Mass Spectrom. 1995; 30:339–347.

14. Iavarone AT, Jurchen JC, Williams ER. Effects of solvent on the maximum charge state and charge state distribution of protein ions produced by electrospray ionization. J. Am. Soc. Mass Spectrom. 2000; 11:976–985. [PubMed: 11073261]

15. Thomson BA. Declustering and fragmentation of protein ions from an electrospray ion source. J. Am. Soc. Mass Spectrom. 1997; 8:1053–1058.

16. Benkestock K, Sundqvist G, Edlund PO, Roeraade J. Influence of droplet size, capillary-cone distance and selected instrumental parameters for the analysis of noncovalent protein–ligand complexes by nanoelectrospray ionization mass spectrometry. J. Mass Spectrom. 2004; 39:1059–1067. [PubMed: 15386746]

17. Iavarone AT, Jurchen JC, Williams ER. Supercharged protein and peptide ions formed by electrospray ionization. Anal. Chem. 2001; 73:1455–1460. [PubMed: 11321294]

18. Iavarone AT, Williams ER. Supercharging in electrospray ionization: Effects on signal and charge. Int. J. Mass Spectrom. 2002; 219:63–72.

19. Iavarone AT, Williams ER. Mechanism of charging and supercharging molecules in electrospray ionization. J. Am. Chem. Soc. 2003; 125:2319–2327. [PubMed: 12590562]

20. Shvartsburg AA, Jones RC. Attachment of metal trications to peptides. J. Am. Soc. Mass Spectrom. 2004; 15:406–408. [PubMed: 14998543]

21. Liu HC, Hakansson K. Divalent metal ion-peptide interactions probed by electron capture dissociation of trications. J. Am. Soc. Mass Spectrom. 2006; 17:1731–1741. [PubMed: 16952459]

22. Chen XF, Fung YME, Chan WYK, Wong PS, Yeung HS, Chan TWD. Transition metal ions: Charge carriers that mediate the electron capture dissociation pathways of peptides. J. Am. Soc. Mass Spectrom. 2011; 22:2232–2245. [PubMed: 21952786]

23. Mosely JA, Murray BS, Parker D. Electron-capture dissociation and collision-induced dissociation of lanthanide metal–ligand complexes and lanthanide metal–ligand complexes bound to phosphopeptides. Eur. J. Mass Spectrom. 2009; 15:145–155.

24. Lomeli SH, Yin S, Loo RRO, Loo JA. Increasing charge while preserving noncovalent protein complexes for ESI-MS. J. Am. Soc. Mass Spectrom. 2009; 20:593–596. [PubMed: 19101165]

25. Lomeli SH, Peng IX, Yin S, Loo RRO, Loo JA. New reagents for increasing ESI multiple charging of proteins and protein complexes. J. Am. Soc. Mass Spectrom. 2010; 21:127–131. [PubMed: 19854660]

26. Sterling HJ, Williams ER. Origin of supercharging in electrospray ionization of noncovalent complexes from aqueous solution. J. Am. Soc. Mass Spectrom. 2009; 20:1933–1943. [PubMed: 19682923]

27. Sterling HJ, Kintzer AF, Feld GK, Cassou CA, Krantz BA, Williams ER. Supercharging protein complexes from aqueous solution disrupts their native conformations. J. Am. Soc. Mass Spectrom. 2012; 23:191–200. [PubMed: 22161509]

28. Sterling HJ, Cassou CA, Trnka MJ, Burlingame AL, Krantz BA, Williams ER. The role of conformational flexibility on protein supercharging in native electrospray ionization. Phys. Chem. Chem. Phys. 2011; 13:18288–18296. [PubMed: 21399817]

29. Sterling HJ, Daly MP, Feld GK, Thoren KL, Kintzer AF, Krantz BA, Williams ER. Effects of supercharging reagents on noncovalent complex structure in electrospray ionization from aqueous solutions. J. Am. Soc. Mass Spectrom. 2010; 21:1762–1774. [PubMed: 20673639]

30. Sterling HJ, Williams ER. Real-time hydrogen/deuterium exchange kinetics via supercharged electrospray ionization tandem mass spectrometry. Anal. Chem. 2010; 82:9050–9057.

31. Sterling HJ, Prell JS, Cassou CA, Williams ER. Protein conformation and supercharging with DMSO from aqueous solution. J. Am. Soc. Mass Spectrom. 2011; 22:1178–1186. [PubMed: 21953100]

32. Grimm RL, Beauchamp JL. Evaporation and discharge dynamics of highly charged multicomponent droplets generated by electrospray ionization. J. Phys. Chem. A. 2010; 114:1411–1419. [PubMed: 19848399]

33. Douglass KA, Venter AR. Investigating the role of adducts in protein supercharging with sulfolane. J. Am. Soc. Mass Spectrom. 2012; 23:489–497. [PubMed: 22219044]

34. Hogan CJ, Loo RRO, Loo JA, de la Mora JF. Ion mobility-mass spectrometry of phosphorylase b ions generated with supercharging reagents but in charge-reducing buffer. Phys. Chem. Chem. Phys. 2010; 12:13476–13483. [PubMed: 20877871]

35. Sze SK, Ge Y, Oh H, McLafferty FW. Top-down mass spectrometry of a 29-kDa protein for characterization of any posttranslational modification to within one residue. Proc. Natl. Acad. Sci. U. S. A. 2002; 99:1774–1779. [PubMed: 11842225]

36. Sheng Y, Loo JA. Top-down mass spectrometry of supercharged native protein–ligand complexes. Int. J. Mass Spectrom. 2011; 300:118–122. [PubMed: 21499519]

37. Valeja SG, Tipton JD, Emmett MR, Marshall AG. New reagents for enhanced liquid chromatographic separation and charging of intact protein ions for electrospray ionization mass spectrometry. Anal. Chem. 2010; 82:7515–7519. [PubMed: 20704305]

38. Iavarone AT, Williams ER. Collisionally activated dissociation of supercharged proteins formed by electrospray ionization. Anal. Chem. 2003; 75:4525–4533. [PubMed: 14632060]

39. Madsen JA, Brodbelt JS. Comparison of infrared multiphoton dissociation and collision-induced dissociation of supercharged peptides in ion traps. J. Am. Soc. Mass Spectrom. 2009; 20:349–358. [PubMed: 19036605]

40. Breuker K, Oh HB, Horn DM, Cerda BA, McLafferty FW. Detailed unfolding and folding of gaseous ubiquitin ions characterized by electron capture dissociation. J. Am. Chem. Soc. 2002; 124:6407–6420. [PubMed: 12033872]

41. Breuker K, Oh HB, Lin C, Carpenter BK, McLafferty FW. Nonergodic and conformational control of the electron capture dissociation of protein cations. Proc. Natl. Acad. Sci. U. S. A. 2004; 101:14011–14016. [PubMed: 15381764]

42. Kharlamova A, Prentice BM, Huang TY, McLuckey SA. Electrospray droplet exposure to gaseous acids for the manipulation of protein charge state distributions. Anal. Chem. 2010; 82:7422–7429. [PubMed: 20712348]

43. Sterling HJ, Cassou CA, Susa AC, Williams ER. Electrothermal supercharging of proteins in native electrospray ionization. Anal. Chem. 2012; 84:3795–3801. [PubMed: 22409200]

44. Jurchen JC, Williams ER. Origin of asymmetric charge partitioning in the dissociation of gas-phase protein homodimers. J. Am. Chem. Soc. 2003; 125:2817–2826. [PubMed: 12603172]

45. Marshall AG, Wang TL, Ricca TL. Tailored excitation for fourier transform ion cyclotron resonance mass spectrometry. J. Am. Chem. Soc. 1985; 107:7893–7897.

46. Schnier PD, Jurchen JC, Williams ER. The effective temperature of peptide ions dissociated by sustained off-resonance irradiation collisional activation in fourier transform mass spectrometry. J. Phys. Chem. B. 1999; 103:737–745. [PubMed: 16614752]

47. Bush MF, Hall Z, Giles K, Hoyes J, Robinson CV, Ruotolo BT. Collision cross sections of proteins and their complexes: A calibration framework and database for gas-phase structural biology. Anal. Chem. 2010; 82:9557–9565. [PubMed: 20979392]

48. Ruotolo BT, Benesch JLP, Sandercock AM, Hyung SJ, Robinson CV. Ion mobility-mass spectrometry analysis of large protein complexes. Nat. Protoc. 2008; 3:1139–1152. [PubMed: 18600219]

49. Iavarone AT, Udekwu OA, Williams ER. Buffer loading for counteracting metal salt-induced signal suppression in electrospray ionization. Anal. Chem. 2004; 76:3944–3950. [PubMed: 15253628]

50. Pan P, Gunawardena HP, Xia Y, McLuckey SA. Nanoelectrospray ionization of protein mixtures: Solution pH and protein pI. Anal. Chem. 2004; 76:1165–1174. [PubMed: 14961751]

51. Brutscher B, Bruschweiler R, Ernst RR. Backbone dynamics and structural characterization of the partially folded a state of ubiquitin by H-1, C-13, and N-15 nuclear magnetic resonance spectroscopy. Biochemistry. 1997; 36:13043–13053. [PubMed: 9335566]

52. Myung S, Badman ER, Lee YJ, Clemmer DE. Structural transitions of electrosprayed ubiquitin ions stored in an ion trap over 10ms to 30s. J. Phys. Chem. A. 2002; 106:9976–9982.

53. Hoaglund CS, Valentine SJ, Sporleder CR, Reilly JP, Clemmer DE. Three-dimensional ion mobility TOF-MS analysis of electrosprayed biomolecules. Anal. Chem. 1998; 70:2236–2242. [PubMed: 9624897]

54. Prell JS, Flick TG, Oomens J, Berden G, Williams ER. Coordination of trivalent metal cations to peptides: Results from IRMPD spectroscopy and theory. J. Phys. Chem. 2010; 114:854–860.

55. Robinson EW, Leib RD, Williams ER. The role of conformation on electron capture dissociation of ubiquitin. J. Am. Soc. Mass Spectrom. 2006; 17:1469–1479. [PubMed: 16890453]

56. Miladinovi SM, Fornelli L, Lu Y, Piech KM, Girault HH, Tsybin YO. In-spray supercharging of peptides and proteins in electrospray ionization mass spectrometry. Anal. Chem. 2012; 84:4647–4651. [PubMed: 22571167]
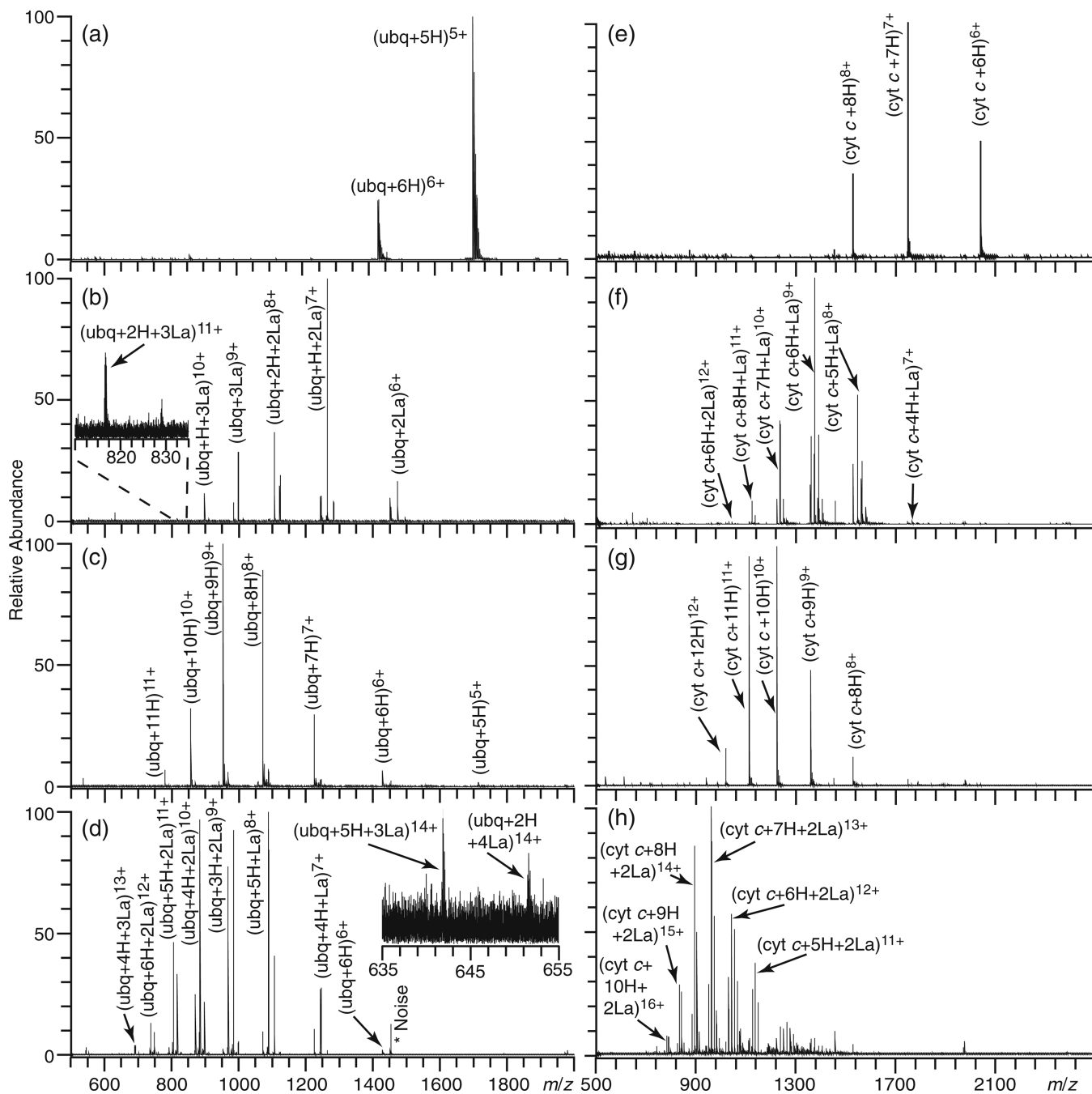
Figure 1.
ESI mass spectra of aqueous solutions of 10 μM ubiquitin or cytochrome c in 5 mM ammonium acetate containing **(a)** and **(e)** no additives, **(b)** and **(f)** 1.0 mM LaCl$_3$, **(c)** and **(g)** 1.0 % m-NBA, or **(d)** and **(h)** 1.0 mM LaCl$_3$, and 1.0 % m-NBA, respectively
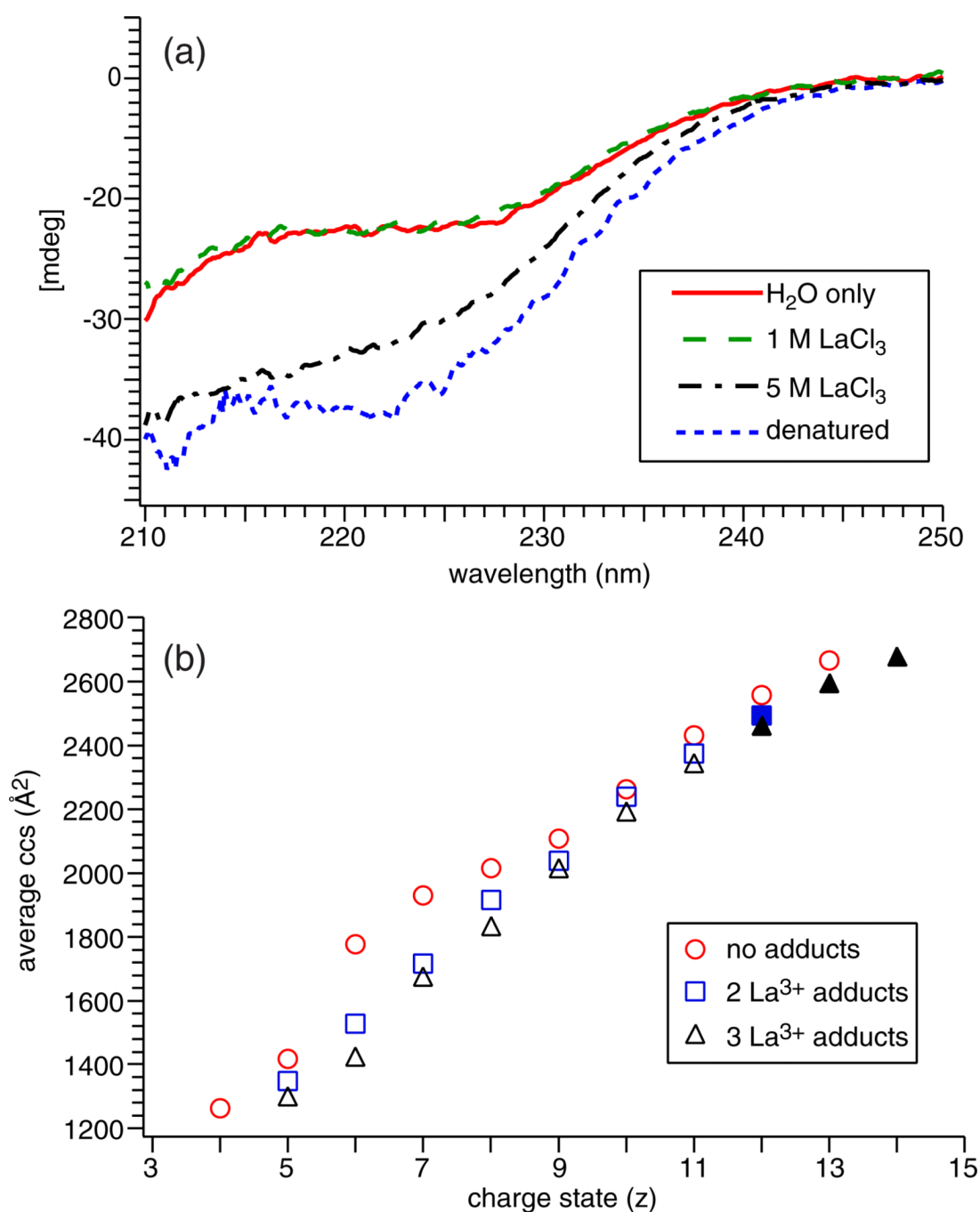
Figure 2.
(a) Circular dichroism spectra between 210 to 250 nm for 20 μM ubiquitin in 5 mM ammonium acetate, 1 M LaCl$_3$ (5 mM ammonium acetate), 5 M LaCl$_3$ (5 mM ammonium acetate), or 48.5/48.5/3.0 methanol/water/acetic acid (vol/vol/vol) (denatured). **(b)** Average collision cross sections as a function of ion charge state for ubiquitin with no adducts from a denatured solution (○) and from an aqueous ammonium acetate solution ( ) without LaCl$_3$, and with two (□) or three (Δ) La^{3+} adducts from an aqueous ammonium acetate solution containing 1.0 mM LaCl$_3$. Filled symbols are ubiquitin ions formed from an aqueous ammonium acetate solution containing LaCl$_3$ and *m*-NBA
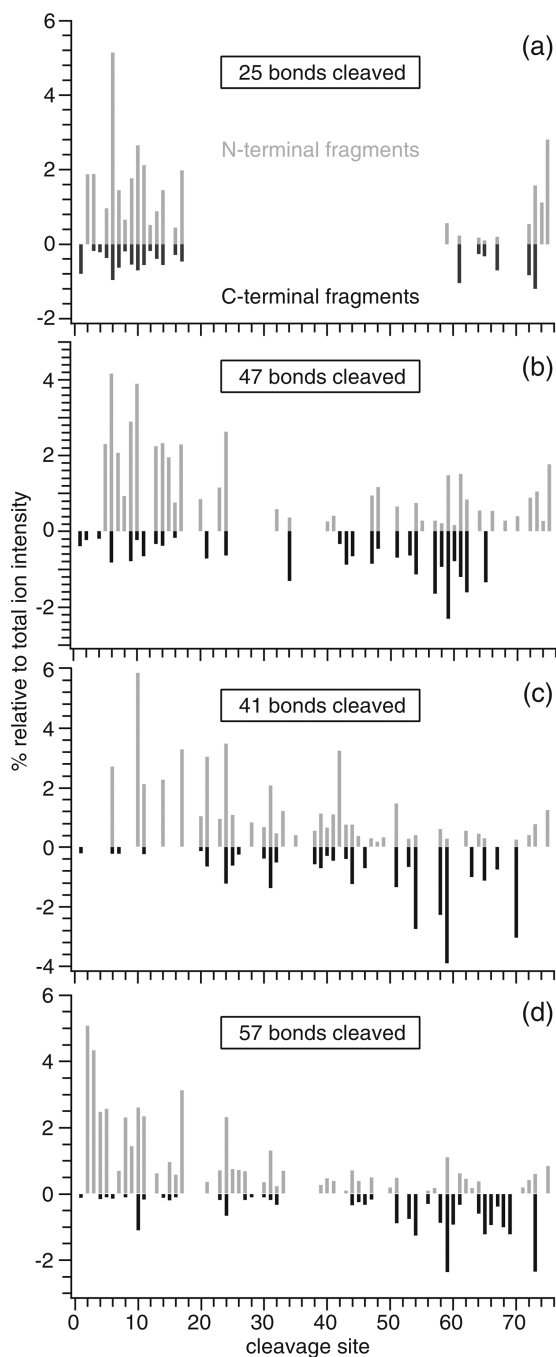
Figure 3.
Relative ECD fragment ion abundances at each cleavage site for **(a)** (ubiquitin+6 H)$^{6+}$, **(b)** (ubiquitin+3La)$^{9+}$, **(c)** (ubiquitin+10 H)$^{10+}$, and **(d)** (ubiquitin+9 H+La)$^{12+}$; N-terminal and C-terminal fragments are represented as positive (grey) and negative (black) values, respectively
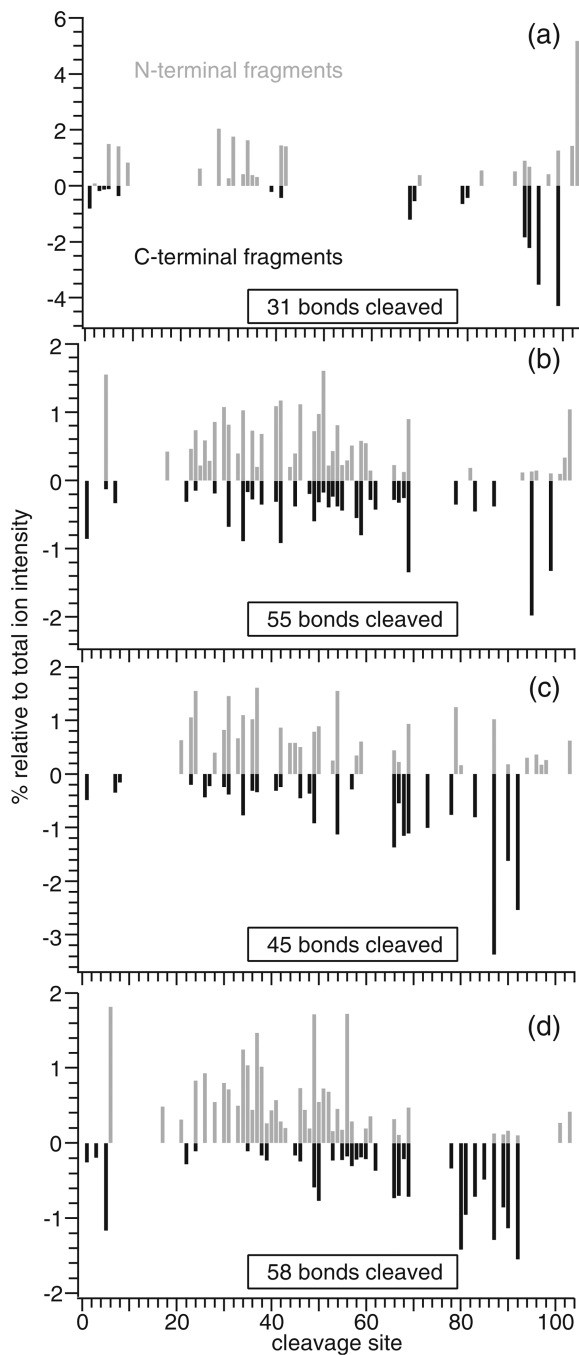
Figure 4.
Relative ECD fragment ion abundances at each cleavage site for **(a)** (cytochrome c+8 H)$^{8+}$, **(b)** (cytochrome c+7 H+La)$^{10+}$, **(c)** (cytochrome c+12 H)$^{12+}$, and **(d)** (cytochrome c+11 H +La)$^{14+}$; N-terminal and C-terminal fragments are represented as positive (grey) and negative (black) values, respectively
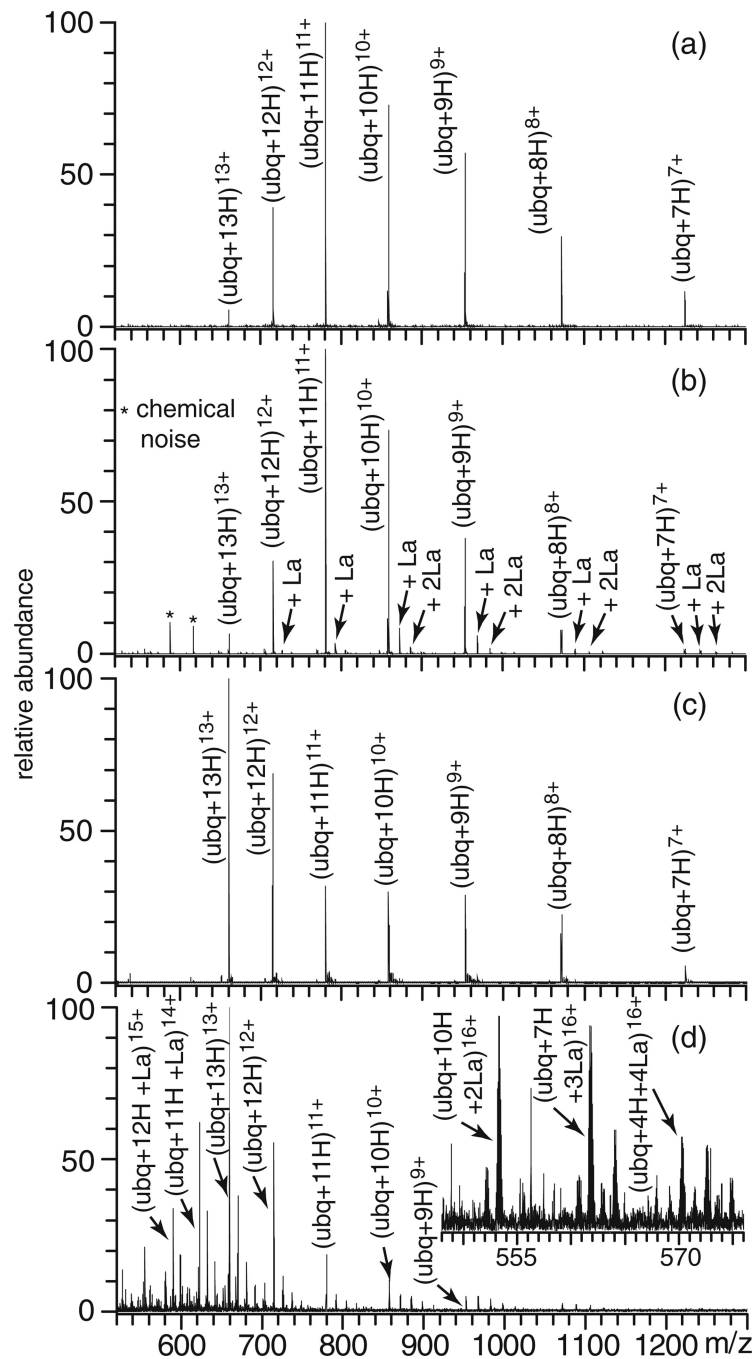
Figure 5.
ESI mass spectra of 10 μM ubiquitin in 48.5/48.5/3.0 methanol/water/acetic acid (vol/vol/
vol) containing **(a)** no additives, **(b)** 1.0 mM LaCl₃, **(c)** 1.0 % *m*-NBA, or **(d)** 1.0 mM LaCl₃
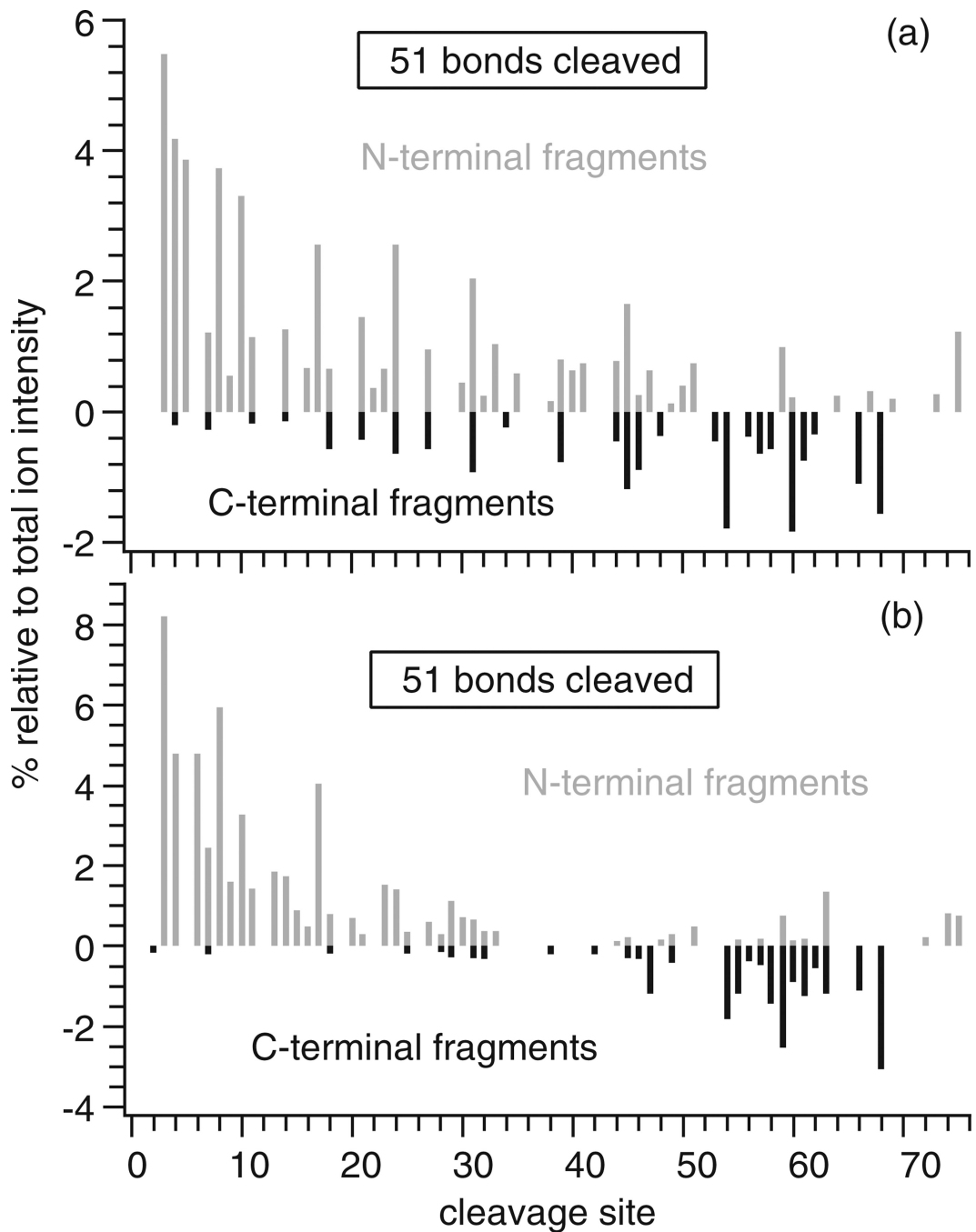and 1.0 % *m*-NBA

Figure 6.
Relative ECD fragment ion abundances at each cleavage site for **(a)** (ubiquitin+13 H)$^{13+}$ and **(b)** (ubiquitin+11 H+La)$^{14+}$; N-terminal and C-terminal fragments are represented as positive (grey) and negative (black) values, respectively

Table 1

The Most Abundant Ion S/N and Total Ion Abundance S/N of Ubiquitin, Cytochrome *c*, or Lysozyme from the ESI Mass Spectra of Aqueous Solutions (5 mM Ammonium Acetate) with and without Supercharging Additives

Protein	Additive	Most abundant ion	Most abundant ion S/N	Total ion abundance S/N
Ubiquitin	None	(ubiquitin+5H)$^{5+}$	9068	27,256
	1.0 % m-NBA	(ubiquitin+9H)$^{9+}$	8380	25,524
	1.0 mM LaCI$_3$	(ubiquitin+H+2La)$^{7+}$	5487	23,713
	1.0 % m-NBA & 1.0 mM LaCI$_3$	(ubiquitin+4H+2La)$^{10+}$	955	9734
Cytochrome *c* (cyt *c*)	None	(cyt *c*+7H)$^{7+}$	7943	17,475
	1.0 % m-NBA	(cyt *c*+10H)$^{10+}$	8332	23,330
	1.0 mM LaCI$_3$	(cyt *c*+6H+La)$^{9+}$	6896	17,930
	1.0 % m-NBA & 1.0 mM LaCI$_3$	(cyt *c*+7H+2La)$^{13+}$	2786	7244
Lysozyme (lys)	None	(lys+8H)$^{8+}$	12,345	17,283
	1.0 % m-NBA	(lys+11H)$^{11+}$	10,452	24,040
	1.0 mM LaCI$_3$	(lys+7H+La)$^{10+}$	7782	17,439
	1.0 % m-NBA & 1.0 mM LaCI$_3$	(lys+11H)$^{11+}$	5481	13,703

Table 2

Average Collision Cross Section (Å^2), % Sequence Coverage, Electron Capture Efficiency, and Fragmentation Efficiency for Ions of Ubiquitin, Cytochrome c, and Lysozyme

Protein	Precursor	Avg. ccs (Å^2)	% Sequence coverage	% Eff$_{EC}$	% Eff$_{frag}$
Ubiquitin	$(\text{ubq}+6\text{H})^{6+}$	1776	33 %	84.3 % ± 0.3 %	64.7 % ± 1.1 %
	$(\text{ubq}+2\text{La})^{6+}$	1527	25 %	77.2 % ± 0.7 %	45.9 % ± 0.8 %
	$(\text{ubq}+9\text{H})^{9+}$	2108	59 %	91.9 % ± 0.6 %	89.5 % ± 0.6 %
	$(\text{ubq}+3\text{La})^{9+}$	2014	63 %	93.2 % ± 0.9 %	85.8 % ± 1.7 %
	$(\text{ubq}+10\text{H})^{10+}$	2263	55 %	92.4 %	89.8 %
	$(\text{ubq}+9\text{H}+\text{La})^{12+}$	2526	76 %	93.9 %	87.5 %
Cytochrome c	$(\text{cyt } c+8\text{H})^{8+}$	2472	30 %	87.4 %	56.9 %
	$(\text{cyt } c+\text{La}+7\text{H})^{10+}$	2718	53 %	88.4 %	66.9 %
	$(\text{cyt } c+12\text{H})^{12+}$	3000	43 %	89.8 %	71.8 %
	$(\text{cyt } c+\text{La}+11\text{H})^{14+}$	3194	56 %	94.5 %	87.7 %
Lysozyme	$(\text{lys}+10\text{H})^{14+}$	2692	-	72.7 % ± 0.6 %	-
	$(\text{lys}+\text{La}+7\text{H})^{10+}$	2692	-	74.8 % ± 0.8 %	-